REPRINTED WITH PERMISSION FROM © IEEE Transactions on Nuclear Science, Vol.NS-23, No.1, February 1976

PSEUDO-GAUSSIAN TRANSFER FUNCTIONS WITH SUPERLATIVE BASELINE RECOVERY

C. H. Mosher
Nuclear Equipment Corporation
963A Industrial Road
San Carlos, CA 94070

Summary

The transfer function comprised of (2n+1) poles unit spaced in the ω direction on the line s=-D in the s plane is analyzed in the time domain and shown to have the response $F_n(t)=C_n e^{-Dt}\sin^{2n}(t/2)$, providing a clean pseudo-gaussian pulse. If D=1.5, the afterpulses are theoretically down by about a factor of 8×10^{-5} and are experimentally acceptable. Experimentally, such an analog signal processor (D=1.5, n=3, unit time = 20 us.) shows excellent shift vs. input rate.

Introduction

In energy dispersive spectrometry, it is common to follow the pulse shaping amplifier with a baseline restorer, which can function well only to the extent that the amplifier output does indeed return to the baseline after the pulse. Generally, the peak of the waveform in the time domain is taken to be the "signal" while noise integrals are most easily evaluated in the frequency domain; hence it is desirable for the transfer function to be simultaneously characterized in both domains. Since the amplifier phase function does not influence the noise integrals in the frequency domain in any way, it is desirable that the transfer function be "linear phase" so that the waveform will peak at the highest possible amplitude by virtue of having all fourier components in phase at that time.

Theoretical Discussion

Guillemin[1] suggested as a starting point of such a linear phase approximation and synthesis problem an array of poles such as shown in Figure 1, which is a

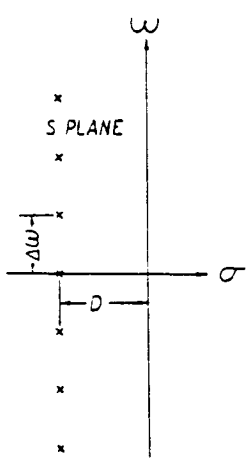

Fig. 1. Pole pattern in s plane.

low-pass filter. He analyzed this transfer function in the frequency domain, where it was visualized as an equal ripple linear phase approximant requiring "end correction" for optimization over a band in the frequency domain. Such end correction would be obtained by moving or adding (extra) poles at the end of the array to increase the delay at the high frequency end of the band, these moved or added poles generally not having the same periodicity and/or damping as the main array.

Consider the implications of such end correction in the time domain: the prototype array has all poles simple, of the same damping, and at frequencies that are all harmonics of the basic oscillatory frequency $\Delta\omega$. If there are k poles, then at t=0 the response and its first (k-2) derivatives are zero, and this boundary condition will repeat at $t=2\pi/\Delta\omega$, $4\pi/\Delta\omega$, etc. Similarly, the absolute amplitude of each pulse will be $e^{-2\pi D/\Delta\omega}$ smaller than that of the preceding pulse. There are no terms of the form t cos(t), te^{-t}, or t sin(t). Any addition or modification would destroy one or more of these simple but useful properties. Therefore, the prototype array was analyzed in the time domain to determine to what extent it might be useful for pulse shaping in energy dispersive spectrometry.

The transfer function of a pulsed optical feedback preamplifier is a simple pole at s=o with its zero at s=oo. This can be compensated in the pulse shaping amplifier by placing one zero at s=0 instead of leaving them all at s=oo, and hence need not be considered further here.

The presence of a pole on the real axis greatly simplifies the implementation of a fine gain control; the case of an even number of poles at half integer frequencies will give qualitatively similar results but is of less practical interest.

Derivation of F(t)

The transfer function for (2n+1) poles, normalized to unity gain at low frequencies and to $\Delta\omega=1$, is

$$f_n(s)=\frac{D\prod_{k=1}^{n}(D^2+k^2)}{(s+D)\prod_{k=1}^{n}((s+D)^2+k^2)}$$

By comparing its expansion term-by-term with that of an ideal gaussian, the equivalent ideal gaussian delay and σ_t can be estimated to be

$$\text{DELAY} = \frac{1}{D} + \sum_{k=1}^{n}\frac{2D}{D^2+k^2}$$

and

$$\sigma_t = \frac{1}{D^2} + \sum_{k=1}^{n}\frac{D^2-k^2}{(D^2+k^2)^2}$$

Those poles with k greater than D increase the delay but decrease σ_t. Expanding f(s) in partial fractions[2] and transforming into the time domain gives

$$F_n(t)=\left\{D\prod_{k=1}^{n}(D^2+k^2)\right\}e^{-Dt}\left\{\frac{1}{(n!)^2}+2\sum_{k=1}^{n}\frac{(-1)^k\cos(kt)}{(n-k)!(n+k)!}\right\}$$

as a sum. It was noted through computing and graphing this sum that it could be expressed in a simpler form,

$$F_n(t)=\left\{D\prod_{k=1}^{n}(D^2+k^2)\right\}e^{-Dt}\left\{\frac{2^{2n}}{(2n)!}\sin^{2n}(t/2)\right\}$$

or

$$F_n(t) = C_n e^{-Dt}\sin^{2n}(t/2)$$

with

$$C_n = \frac{2^{2n}}{(2n)!}\prod_{k=1}^{n}(D^2+k^2)$$

as is easily proved by induction in n. By differentiating this with regard to t, the peak can be located to be at

$$t_p = 2\tan^{-1}(n/D)$$

This expression is exact and reveals the very approximate nature of the delay estimate above.

Figure 2 shows $F_n(t)$ for n=1 to 5, with D=1.5,

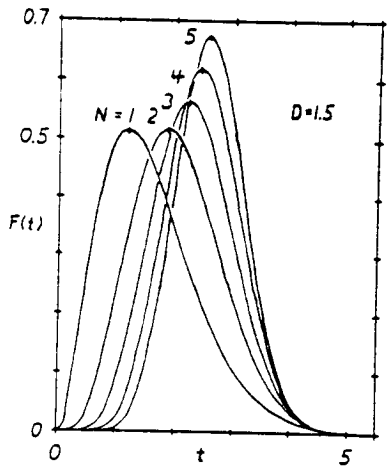

Fig. 2. Plot of $F_n(t)$ for D=1.5, n=1 to 5.

and illustrates the effect mentioned above of poles with frequencies greater than D sharpening the pulse even though they delay it. The peaks have been marked with a pip. Figure 3 shows noise, as theoretical

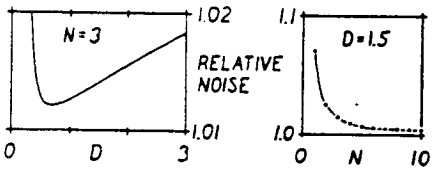

Fig. 3. Noise vs. n, D.

pulser fwhm normalized against an optimum ideal gaussian, as a function of n and D. Note that diminishing returns set in at moderate n and there is very little resolution penalty to using large values of D. Increasing D and/or n does increase dead time for a given σ_t, however. The noise integrals were done numerically in the frequency domain.

Experimental Results

An analog signal processor was built using the n=3, D=1.5 design normalized to 20 microsecond unit time. Figure 4 shows the stage configuration used for

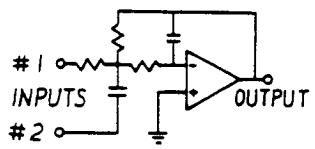

Figure 4. Stage configuration for complex pole pair.

the complex pole pairs. The unused input should be grounded. Input #1 puts both zeroes at s=∞, while input #2 puts one zero at s=0 to realize a "differentiating" stage. Element values were not corrected for finite operational amplifier gains or for finite capacitor Q's. Resistor tolerances were 1%, and capacitor tolerances were 3 or 5% depending on value. Figures 5 and 6 show its response at 20 μs/div and

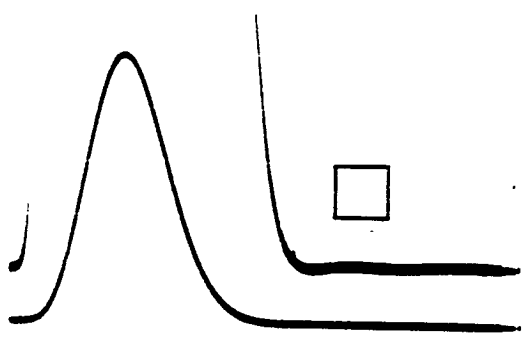

Fig. 5. Experimental F(t), 2v/div and 20 mv/div x 20 μs/div.

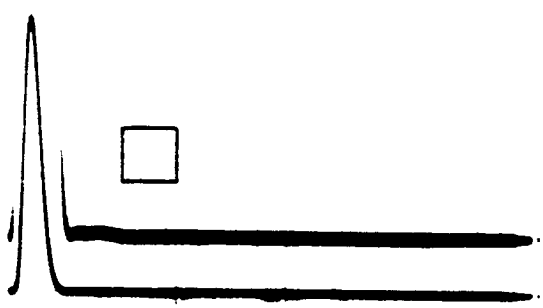

Fig. 6. Experimental F(t), 2v/div and 20 mv/div x 100 μs/div.

100 μs/div respectively. The vertical scales are 20 mv/div (top trace) and 2 v/div (bottom trace). It was found that the first afterpulse could be observed if the scope was protected from overloading by an interposed boxcar gate. Figure 6 shows the first afterpulse to be of about 2 mv amplitude, i.e. about 2×10^{-4} of the main pulse, rather than the $e^{-3\pi} = 8 \times 10^{-5}$ ideal value. The effective dead time for pileup of this amplifier is about 110 μs, providing a maximum output rate above 3 kHz at an input rate of about 9 kHz. Figure 7 shows MnKα line shift vs.

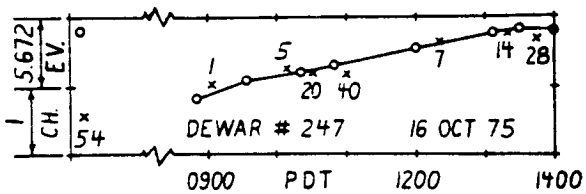

Fig. 7. Shift vs. time and input rate, MnKα .

time and input rate. The circles are spectra at a 10 kHz input rate, and are repeated so that time and temperature effects can be separated from rate effects. The x's are spectra at other rates as labeled. The 10 kHz point in the upper left corner is 1500 PDT on the previous day, and the 54 kHz point in the lower left corner is an overnight run. The departures of the locations at the various rates from the straight lines connecting the 10 kHz points were taken as the rate dependent shifts at these rates. The 10 kHz rate was taken as the reference to permit the fastest possible acquisition of the data. Each spectrum was at least 10^6 counts total with at least 10^4 in the channel at the Kα peak. Peak locations and widths were evaluated using statistical procedures, and were not "eye-balled" off a curve by a favorably biased eye. Because of the substantial non-linear overnight shifts due to the diurnal temperature cycle, the rate dependent shift at 54 kHz can not be estimated from this data. The baseline temperature coefficient of this analog signal processor was +40 μv/°C and the gain temperature coefficient was 0 ±20 ppm/°C, so this diurnal shift must have originated in the ADC or the dewar. Figure 8 shows shift vs. rate up to 40 kHz and resolution

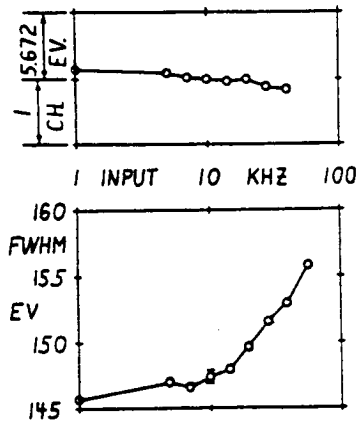

Fig. 8. Shift and resolution vs. input rate, MnKα .

(fwhm) up to 54 kHz. The bars on the 10 kHz point show the ± one standard deviation range of these repeated runs.

Conclusion

The utility of a class of pulse shaping transfer functions, not previously well know in the energy dispersive spectrometry field, and easily characterized in both the frequency and time domains, has been demonstrated theoretically and experimentally.

References

1) Ernst A. Guillemin, Synthesis of Passive Networks. John Wiley & Sons, Inc., 1957, pp. 639-642.

2) Ruel V. Churchill, Operational Mathematics. New York, McGraw-Hill Book Company, Inc., 1958, pp. 57-59.